Since January 2020 Elsevier has created a COVID-19 resource centre with free information in English and Mandarin on the novel coronavirus COVID-19. The COVID-19 resource centre is hosted on Elsevier Connect, the company's public news and information website.

Biosensors and Bioelectronics 185 (2021) 113177

Contents lists available at ScienceDirect

Biosensors and Bioelectronics

journal homepage: http://www.elsevier.com/locate/bios

Short communication

Ultra-fast and recyclable DNA biosensor for point-of-care detection of SARS-CoV-2 (COVID-19)

Chuljin Hwang [a], Nakkyun Park [a], Eun Seong Kim [b], Miran Kim [c], Su Dong Kim [d], Sungjun Park [e,*], Nam Young Kim [b,d,**], Joo Hee Kim [a,d,***]

[a] College of Pharmacy, Ajou University, Suwon 16499, South Korea
[b] Electronic Engineering, Kwangwoon University, Seoul 01897, South Korea
[c] Ajou University School of Medicine, Suwon 16499, South Korea
[d] Graduate School of Clinical Pharmacy and Pharmaceutics, Ajou University, Suwon,16499, South Korea
[e] Department of Electrical and Computer Engineering, Ajou University, Suwon 16499, South Korea

ARTICLE INFO

Keywords:
SARS-CoV-2
Electrochemical DNA detection
Point-of-care diagnostics
Capacitance transducer
Recyclable biosensor

ABSTRACT

Rapid diagnosis and case isolation are pivotal to controlling the current pandemic of severe acute respiratory syndrome coronavirus 2 (SARS-CoV-2). In this study, a label-free DNA capacitive biosensor for the detection of SARS-CoV-2 that demonstrates real-time, low-cost, and high-throughput screening of nucleic acid samples is presented. Our novel biosensor composed of the interdigitated platinum/titanium electrodes on the glass substrate can detect the hybridization of analyte DNA with probe DNA. The hybridization signals of specific DNA sequences were verified through exhaustive physicochemical analytical techniques such as Fourier transform infrared (FT-IR) spectrometry, contact-angle analysis, and capacitance-frequency measurements. For a single-step hybridized reaction, the fabricated kit exhibited significant sensitivity (capacitance change, $\Delta C = \sim 2$ nF) in detecting the conserved region of the SARS-CoV-2 RNA-dependent RNA polymerase (RdRp) gene with high sensitivity of 0.843 nF/nM. In addition to capacitive measurements, this selective detection was confirmed by the fluorescence image and intensity from a SARS-CoV-2 gene labeled with a fluorescent dye. We also demonstrated that the kits are recyclable by surface ozone treatment using UV irradiation. Thus, these kits could potentially be applied to various types of label-free DNA, thereby acting as rapid, cost-effective biosensors for several diseases.

1. Introduction

Since late December 2019, the novel coronavirus, i.e., severe acute respiratory syndrome coronavirus 2 (SARS-CoV-2) that firstly reported in Wuhan City, China, has been spreading around the world, with thousands of deaths (Islam et al., 2020). Moreover, no vaccine or antiviral agent is currently available. The signs of SARS-CoV-2 infection are highly non-specific, including diarrhea, fever, cough, dyspnea, and viral pneumonia (Cascella et al., 2020). Notably, it is reported that this virus is largely propagated during its incubation period in asymptomatic patients (Rothe et al., 2020). According to a recent model, symptomatic patients should be isolated within 24 h of symptom onset to control the spread of coronavirus disease (COVID-19) (Chowell et al., 2020). Rapid detection and isolation of cases would be most effective in suppressing the escalation of the outbreak. Moreover, it is highly important to build pre-diagnostic platforms to avoid making unnecessary sacrifices.

Currently, the standard diagnostic protocol relies on polymerase chain reaction (PCR) to amplify the required genetic material for the detection of SARS-CoV-2 (Corman et al., 2020). It is a highly sensitive and reliable method but not without limitations. The average turnaround time for test results is 24–72 h, but the lag between sample collection and delivery is unpredictable on a large-scale for the COVID-19 global pandemic. Moreover, it requires well-trained professionals as well as expensive and sophisticated laboratories, instruments, and consumables that significantly limit its widespread use. The number of COVID-19 cases has already exceeded PCR testing capacity due to shortages in test kits, creating a new wave of challenges (Sharfstein et al., 2020). In this context, the implementation of a

* Corresponding author. Department of Electrical and Computer Engineering, Ajou University, 16499, South Korea.
** Corresponding author. Electronic Engineering, Kwangwoon University, 01897, South Korea.
*** Corresponding author. College of Pharmacy, Ajou University, 16499, South Korea.
E-mail addresses: sj0223park@ajou.ac.kr (S. Park), nykim@kw.ac.kr (N.Y. Kim), elisekim@ajou.ac.kr (J.H. Kim).

https://doi.org/10.1016/j.bios.2021.113177
Received 8 December 2020; Received in revised form 17 February 2021; Accepted 14 March 2021
Available online 24 March 2021

low-cost, real-time detection method for the screening of SARS-CoV-2 is of high priority.

Point-of-use diagnostic biosensors are an effective alternative to PCR-based detection because of their simplicity of operation, low-cost, and suitability for mass production (Whitesides, 2006). Among previous biosensors, electrochemical methods have drawn significant attention because of their ease of detection, suitability for miniaturization, flexibility in the sensor size, and controllability of sensitive parameters (Singhal et al., 2018). These biosensors measure the change in electrochemical signal upon hybridization between a biotinylated target DNA and a thiolated DNA probe immobilized on a gold electrode surface. For instance, a biosensor that detects the Ebola virus DNA through an enzyme amplification process has been reported (Ilkhani and Farhad, 2018). Later, the detection of the Middle East respiratory syndrome coronavirus (MERS-CoV) using carbon array electrodes modified with gold nanoparticles was performed using voltammetric immunosensors (Layqah and Eissa, 2019). These sensors were technical in nature, requiring high-grade analytical reagents and materials. Furthermore, additional labeling and signal amplification were required to achieve high-level sensitivity, which may incur additional costs during future miniaturization.

Very recently, a field-effect transistor biosensor for the detection of the SARS-CoV-2 spike protein was successfully constructed (Seo et al., 2020). This device was designed to use SARS-CoV-2 spike antibodies anchored by 1-pyrenebutyric acid N-hydroxysuccinimide ester (PBASE) on graphene channel layers. Despite the advantage of a convenient workflow requiring little sample preparation, this new test by a serological approach was less sensitive than RT-PCR using viral RNA; hence, different materials and platforms need to be explored to improve the signal/noise.

There remain challenges to developing low-cost and rapid sensing platforms for highly sensitive viral detection as the minimal change of molecular hybridization is hard to distinguish in vertical device structures. Therefore, it is important to develop reliable testbeds to identify molecular reactions on a nano-scale interface. In this study, we developed a novel SARS-CoV-2 sensor based on interdigitated electrodes (IDE) that detects label-free hybridization between a probe and target DNA. Their distinct electrical signals resulting from selective hybridization of specific DNA sequences were successfully proved through exhaustive electrical and physicochemical analysis. We hope that our demonstration allows for new possibilities in developing real-time, low-cost, label-free DNA sensors for timely and effective detection of COVID-19.

2. Material and methods

2.1. Reagents and materials

A synthetic SARS-CoV-2 gene and a severe acute respiratory syndrome (SARS)-CoV gene were used for proof of concept. A target sequence was selected from the RNA-dependent RNA polymerase (RdRp) genes specific for SARS-CoV-2 (Corman et al., 2020). The complementary DNA was synthesized via reverse transcription of RdRp gene in the SARS-CoV-2 virus gene and used as the target DNA in this study. The probe DNA was designed to form a stable duplex with the target sequence (Supplementary Table 1). The sequence of a SARS-CoV gene contains four mismatched base pairs with the probe sequence. The probe DNA (5′-Phosphate-GCA TCT CCT GAT GAG GTT CCA CCT G-3′), complementary target analyte (5′-CAG GTG GAA CCT CAT CAG GAG ATG C-3′) and the non-complementary analyte (5′-CCA GGT GGA ACA TCA TCC GGT GAT GC-3′) were purchased from Bionics (Seoul, S. Korea). Sulfuric acid, hydrogen peroxide, and anhydrous ethanol were obtained from Samchun (Seoul, S. Korea). 3-Aminopropyltriethoxysilane (APTES) was purchased from Sigma-Aldrich (St. Louis, MO, USA) and stored in a dry, ventilated place before use. Phosphate-buffered saline (PBS) was purchased from CUREBIO (Seoul, S. Korea). All other reagents and solvents were of analytical grade, and deionized (DI) water (Milli-Q® system, 18.2 MΩ cm, 25 °C) was used throughout the experiments.

2.2. Construction of interdigitated electrode (IDE) on a glass wafer

A 6-inch glass wafer was prepared by sequential cleaning in acetone, isopropyl alcohol, and DI water in an ultrasonic bath for 5 min. After the cleaning process, the glass wafer was blown gently with pressurized nitrogen gas and kept at 70 °C to remove redundant moisture. IDEs were constructed on a glass wafer using a conventional photolithography process. Thick layers (150 nm) of both titanium (Ti) and platinum (Pt) were deposited by e-beam evaporation on to the glass wafer. The Ti layer helps with the adhesion between the Pt and glass substrate. Finally, the wafer was diced into single chips. The channel width was 4100 μm, including the 64 interdigital electrodes, and the channel length was 100 μm, providing a total sensing area of about 13.12 mm^2.

2.3. Surface treatment for DNA hybridization

First, the surface was modified to introduce hydroxyl groups onto the glass surface of the IDE sensors. The sensors were cleaned at 80 °C in a solution of 3:1 concentrated H_2SO_4/H_2O_2 (aq) (hereafter referred to as piranha solution) and then rinsed with DI water to remove the reagents. Then, UV/ozone treatment was conducted for 10 min (UVO Cleaner, model 30, Jelight Company, Inc.), resulting in hydroxyl groups with a surface transformation from hydrophobicity to hydrophilicity (Fan et al., 2019). Second, 5% (v/v) APTES in ethanol was dropped onto the surface and dried to functionalize the amine groups as linker molecules to react with the probe DNA (Jang and Liu, 2009; Syga et al., 2018). Finally, the sensors were rinsed with DI water to remove the adsorbed APTES and dried at room temperature before characterization. The probe DNA was suspended in DI water at a concentration of 5 μM. Then, 10 μL of this solution was dropped onto the sensor and immediately placed in a closed container for 3 h at 60 °C. During the reaction, the probe DNA was immobilized onto the amine-functionalized glass surface via a phosphoramidate linkage through a one-step reaction. After incubation, the sensors were thoroughly rinsed with DI water to remove redundant probe DNA and dried in the container at room temperature. The linkage between APTES and the probe DNA is a covalent bond caused by the molecular reaction between amine and phosphate (Chen et al., 2015). The prepared sensors were stored in a closed container immediately before use.

2.4. Detection of the target analyte

All experiments were performed in quintuplet. First, complementary SARS-CoV-2 cDNA and non-complementary SARS-CoV cDNA were dissolved in DI water and then diluted in PBS to make 5 μM solution. For hybridization, 10 μL of each analyte solution was dropped onto the sensor and incubated for 1 h at 60 °C to reduce non-specific reactions. After this, the sensors were washed individually with DI water to remove non-hybridized DNA and dried at room temperature. The capacitance values were measured in the frequency range of 10 Hz–10^3 Hz, using an impedance analyzer (HIOKI, IM3570) within a few seconds (Mishra et al., 2020). A 500 mV root mean square (RMS) AC voltage was applied across the IDE sensor. All results were collected and statistically analyzed using a paired *t*-test and *p*-value for statistical significance.

2.5. Surface characterization

The surface energy of the hydroxylation onto the glass surface, amine functionalization, and probe DNA immobilization were estimated via contact angle measurements, which were carried out by dispensing DI water onto different chemical surfaces. The side view photograph of the contact angle measurement was taken using a digital camera (Navitar)

and processed with an image analysis software (UNI-CAM). The attenuated total reflection Fourier transform infrared spectroscopy (ATR-FT-IR, Nicolet iS50, Thermo) measurement technique was used to investigate the carbon skeleton (-CH_2) and terminal amine groups (-NH_2) in the APTES anchored to the glass surface. The intensity of fluorescence was confirmed using a fluorescence microscope (EVOS M5000, Thermo) and ELISA reader (Synergy H1, BioTek). The probe DNA immobilization and the hybridization of the target analyte were further validated using fluorescent target capture on the sensor surface.

2.6. Recyclability test

The sensor recyclability was tested by checking the capacitance between bare sensors and hybridized sensors whenever it was reused. The process was repeated five times, and the change in capacitance was measured after each cycle.

3. Results and discussion

3.1. The operational mechanism of SARS-CoV-2 biosensor

Fig. 1A shows a schematic diagram of the sequence of probe DNA using specific mRNA sequences in the SARS-CoV-2 gene and hybridization between the probe DNA and SARS-CoV-2 cDNA. From the RdRp genes specific of SARS-CoV-2 (Corman et al., 2020), a major sequence for probe DNA was selected. As a target DNA experiments, SARS-CoV-2 (complementary DNA with probe DNA) and SARS-CoV gene (non-complementary DNA containing four mismatched base pairs with probe sequence) were synthesized for this study. The photograph of capacitance-frequency (C-f) measurement setup is shown in Supplementary Fig. 1A. By mounting and withdrawing several chips repeatedly, signal detection in reliable and rapid manner can be achieved. Compared to conventional electrode design, our novel IDE design is beneficial due to their larger effective area for detecting biological species and enabling better spatial capability and reactivity (Supplementary Fig. 1B). The interdigitated electrode structure consists of 64 electrode fingers, and the width and length of IDE are 4100 and 100 μm, providing a total sensing area of 13.12 μm^2. After constructing the IDE, surface modification of the glass substrate was conducted, as shown in Fig. 1B. There are various reports on the surface modification of glass substrates with different functional groups for making covalent bonds with DNA. Among the functionalized silane chemistry, APTES is most widely used for DNA immobilization (Albalá et al., 2004; Chen et al., 2015; Olmos et al., 2003; Wang et al., 2006; Watson et al., 2001). The formation of well-defined short-chain functionalized silanes can be achieved under precise control of the reaction time and the concentration of the medium (APTES treatment). Sequentially, the probe DNA immobilization takes place on APTES-modified glass substrates (probe DNA immobilization). The ordered layer of probe DNAs on the surface is a prerequisite to ensure accessibility to the target DNAs (Dufva, 2005). To maximize the number of chemisorbed probe DNA molecules on the surface, a concentration of 5 μM with an incubation time of 3 h was chosen in our experiments because the DNA immobilization is susceptible to the rough surface of the glass, incubation time, and

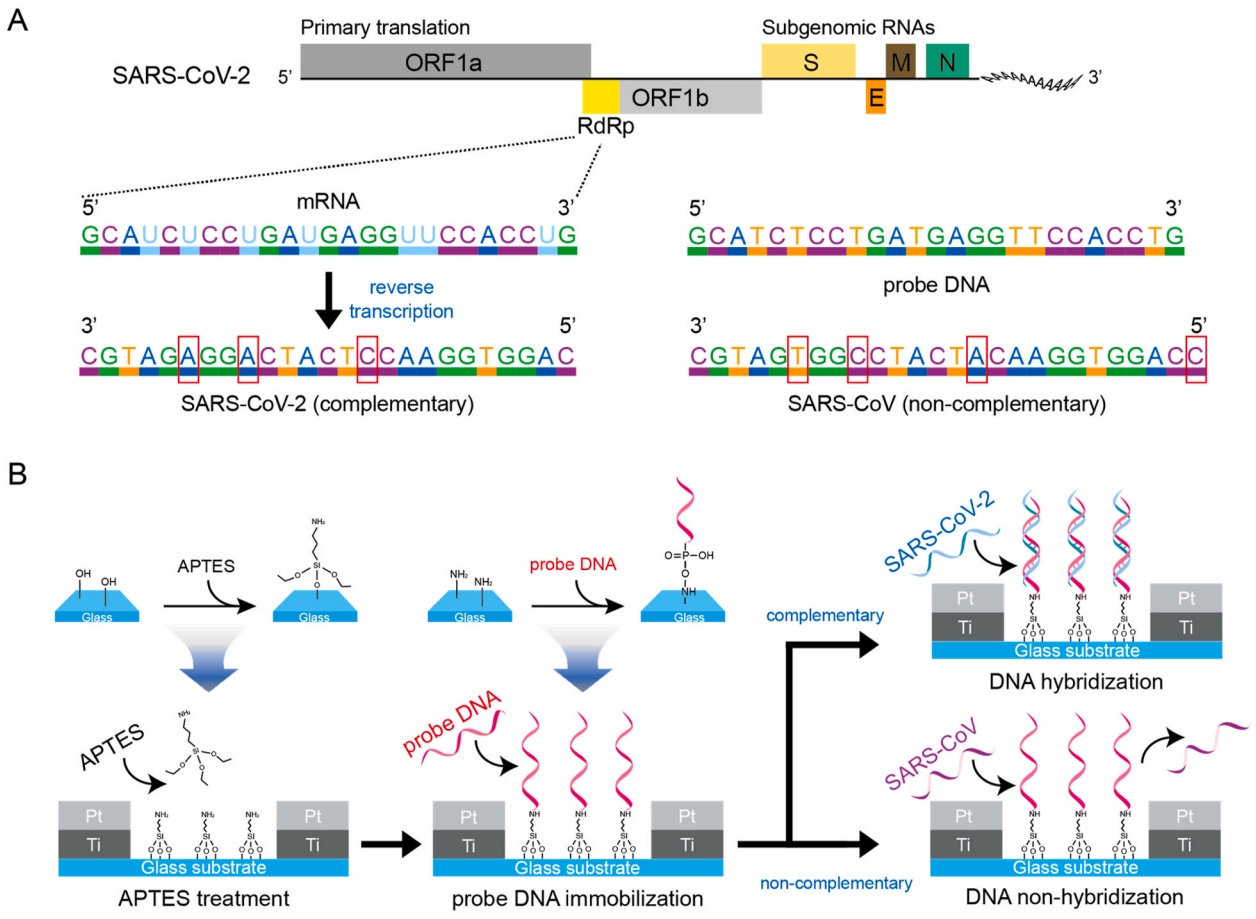

Fig. 1. Operational principal of the IDE biosensor for SARS-CoV-2 cDNA detection. (A) A schematic diagram of the sequence of probe DNA using specific mRNA sequences in the SARS-CoV-2 virus gene and the sequence of complementary DNA using reverse transcription sequence of SARS-CoV-2 mRNA (B) The schematic diagram showing the surface construction process of APTES treatment followed by probe DNA immobilization and the hybridization reaction of analyte DNA with probe DNA for SARS-CoV-2 cDNA detection.

concentration (Rashid and Yusof, 2017). Based on the DNA sequence, the complementary target DNA can be hybridized with the probe DNA to form double-stranded DNA (dsDNA) through hydrogen bonds (DNA hybridization), but the non-complementary SARS-CoV cDNA cannot (DNA non-hybridization). When the target DNA reacts and hybridizes with the probe DNA, the strengthened spatial charge distribution between the electrodes leads to an increase of the capacitance values.

3.2. Physicochemical analysis on the reactive site of the SARS-CoV-2 biosensor

The optimization of the sensor surface for DNA hybridization is crucial to secure both high specificity and sensitivity, which is primarily dependent on the condition of the immobilized probe DNA. During the step-by-step device construction process, physiochemical analysis of the reactive surface was conducted to verify compatibility between the probe and the target DNA. Fig. 2A shows the contact angle measurement of the surface after chemical modification. The contact angle of the bare surface was 45.8°. After piranha and UV/ozone treatment, the contact angle of the hydroxyl-modified surface decreased to an immeasurable value (<3°); this corresponds with previous research (Schrader et al., 2018). The contact angle was increased to 39.4° after APTES treatment, implying that the uniform coverage of the silane molecular layer consisting of exposed free hydrophilic amine groups was achieved. The higher contact angle than 41° would be achieved due to the partial exposure of hydrophobic hydrocarbons and hydrophilic amine functional groups of APTES (Kyaw et al., 2015), indicating fewer binding sites of probe DNA molecules. According to a previous study, the ideal contact angle of 41° was achieved where each Si bond from the APTES molecules was covalently bonded as a tripod structure, leading the amine groups toward the substrate (Kyaw et al., 2015). Therefore, neutral pH was carefully chosen for surface washing treatment after APTES treatment (Supplementary Fig. 2A). Our results indicate that the effective surface of the sensor was successfully modified with hydroxylation, followed by amination. When probe DNA is immobilized onto APTES, the contact angle gradually increased because of the changes in the surface properties from the presence of the DNA (Chaudhary et al., 2014; Elder and Jayaraman, 2013).

To confirm the presence of a chemical reaction at the effective surface, ATR-FT-IR analysis was conducted, as shown in Fig. 2B. ATR-FT-IR is a useful tool for examining functional groups on thin molecular layers with a penetration depth of around 1–2 nm. Effective assembly of the APTES layer on the glass surface was reflected by the presence of a strong absorption peak at 1568 cm^{-1} and 2800-2980 cm^{-1}, indicating N–H (Wang et al., 2014) and C–H stretching (Gunda et al., 2014), respectively. In Fig. 2C, the probe DNA immobilization was successfully verified by producing a strong fluorescence expression. To optimize the stimulus signal frequency, *C-f* electrical characterization was conducted by measuring capacitance values of the bare chip, APTES, probe DNA at frequency ranges from 10 to 10^3 Hz as displayed in Fig. 2D (Wang et al., 2017). At a low frequency of 10 Hz, reliable capacitance changes were observed on each step of the surface modification in our experiment. The values of capacitance decreased rapidly with increases in stimulus frequency. When the frequency applied to the capacitor increases, the capacitive reactance (X_c) decreases because the electrical charge in the internal space between the electrodes can rapidly pass from one to the other electrode at varying frequencies. The capacitive reactance can be expressed by the following equation:

$$Xc = \frac{1}{2\pi fC}$$

Where Xc is capacitive reactance in Ohms, f is frequency in Hertz, and C is capacitance in Farads.

We observed large increases of capacitance values at 10 Hz produced by probe DNA immobilization compared to the bare chip and APTES treatment due to intrinsic property of dielectric constant. Indeed, it is reported that the dielectric constant of functionalized APTES (Macambira et al., 2018) and the complex carbon chain of DNA (Cuervo et al., 2014) is approximately $\varepsilon = 3.57$ and $\varepsilon = \sim 8$, respectively.

3.3. SARS-CoV-2 cDNA sensitivity, identification, and device recyclability

After immobilization of the probe DNA, the sensitivity and specificity of the complementary SARS-CoV-2 target analyte were evaluated. To validate minimum sensitivity of the sensors, different concentration of complementary SARS-CoV-2 target DNA was tested as shown in Fig. 3A. It is confirmed that linear capacitive response for complementary SARS-CoV-2 cDNA (0.843 nF/nM, 10 nM of limit of detection (LoD)) and

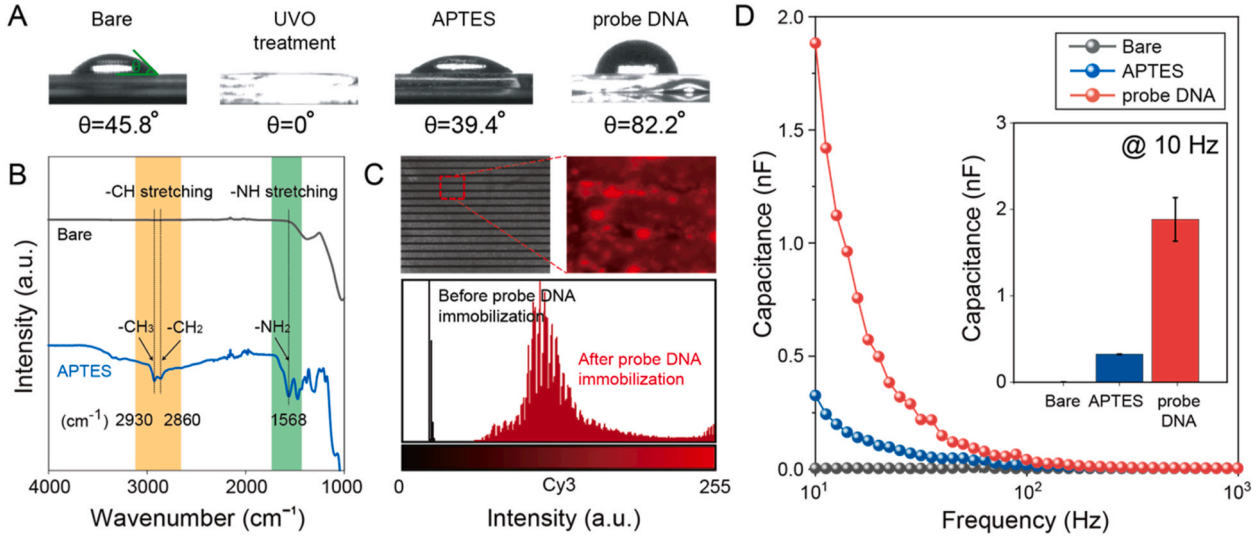

Fig. 2. The physicochemical and electrical validation of the binding-site of the sensor surface. (A) Contact angle changes with surface treatment (from left to right): Bare glass substrate, substrate after UVO treatment, APTES treatment, and probe DNA immobilization (B) ATR-FT-IR spectra for the bare surface (top, black) and the surface after APTES treatment (bottom, blue). The black arrows indicate the (C–H) and (N–H) functional groups of the APTES molecule (C) Fluorescence microscope and histogram of probe DNA immobilization. Strong expression of red fluorescence indicates successful binding between APTES and the probe DNA (D) Capacitance measurement of each experimental step; bare condition (black), after APTES treatment (blue), and after probe DNA immobilization (red).

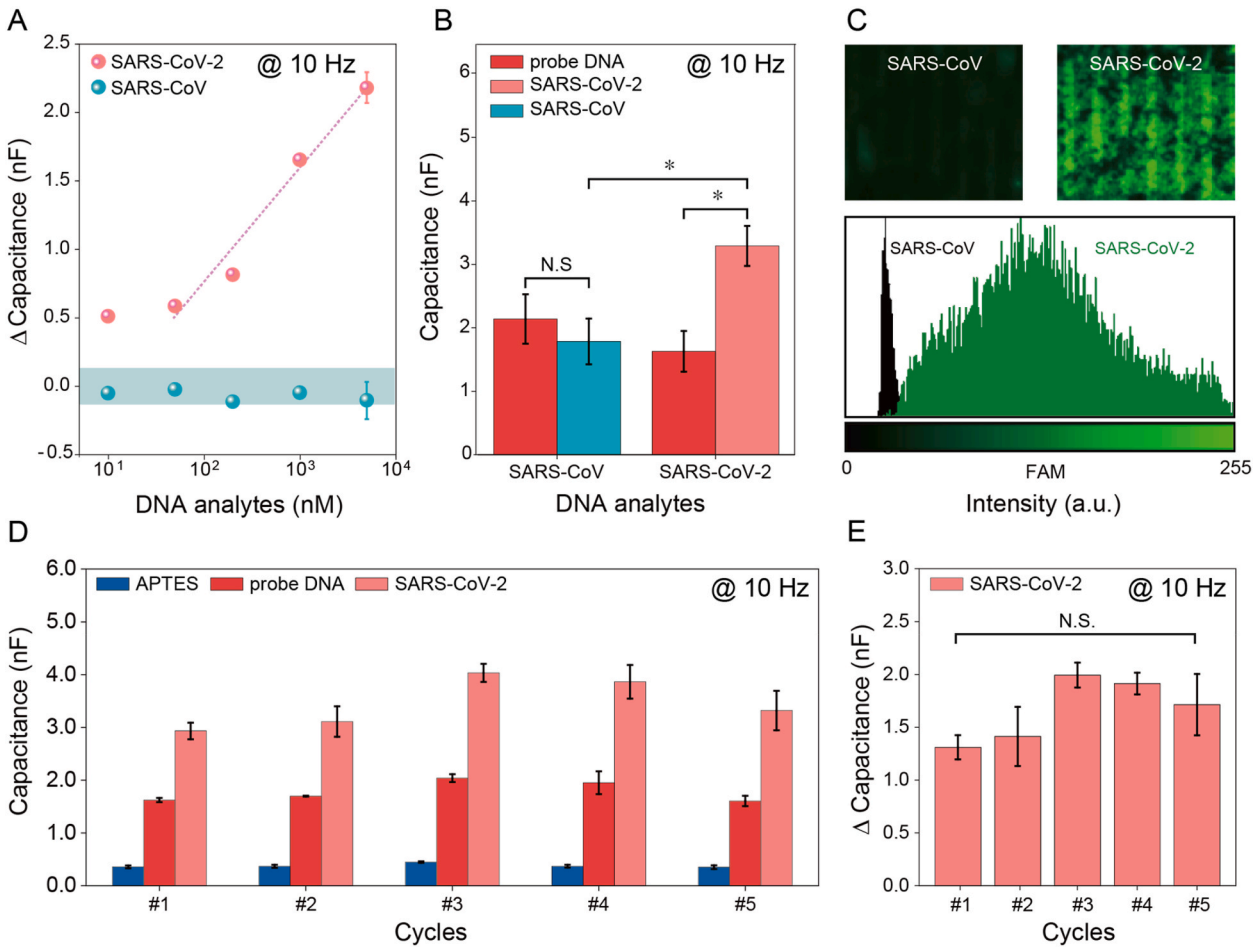

Fig. 3. Sensitivity and recyclability test of SARS-CoV-2 cDNA sensors. (A) The sensitivity was tested by varying the concentration of SARS-CoV-2 (B) Capacitance histogram showing the statistically significant differences between the before and after hybridization of SARS-CoV-2 as well as SARS-CoV (C) Comparative histogram analysis of signal intensity indicating the strong green-colored fluorescent target capture (D) Comparable capacitance values after APTES treatment, probe DNA and SARS-CoV-2 cDNA during the recycle of the three sets of sensors (E) The changes in capacitance values across the recycling indicating the highly sensitive detection of SARS-CoV-2. * indicates "significant, ($p < 0.05$)", N.S indicates "non-significant".

invariant response for non-complementary SARS-CoV cDNA were detected with logarithmic change of target concentration from 5 μM to 10 nM. It is worth to note that our capacitive sensor exhibits prominent sensitivity compared to previously reported electrochemical DNA sensors (Faria and Zucolotto, 2019) and it is validated to be used as point-of-use diagnostic biosensors as long as preconditioning and high-concentration DNA extraction platform on site is well established.

The average change of capacitance values of the sensors incubated with complementary and non-complementary analyte DNAs were evaluated in Fig. 3B. The non-complementary SARS-CoV analyte did not induce a significant capacitance change, whereas the complementary SARS-CoV-2 target analyte exhibited statistically significant increases in capacitance ($\Delta C = \sim 2$ nF), with a narrow statistical distribution ($p < 0.05$). Upon the introduction of the complementary SARS-CoV-2 cDNA, the successful formation of dsDNA was confirmed by the statistically significant increase in capacitance values (Supplementary Fig. 3A). As has been previously demonstrated in the literature, the increase in capacitance occurred when the properties of the dielectric materials between the electrodes changed (Tsouti et al., 2011).

The capture of the target analyte was further validated by measuring the fluorescent signal above the glass surface. As shown in Fig. 3C, the strong green fluorescence revealed the successful hybridization between the SARS-CoV-2 target and the probe DNA. All these results support the specific detection of complementary SARS-CoV-2 cDNA by our sensors.

Finally, a recyclability test was conducted for each experimental cycle, as shown in Fig. 3D and E. By the simple process of piranha cleaning and UV/ozone treatment, the clean glass substrate of the sensors was regenerated without removing the transducers. The piranha solution was used as a denaturing agent to remove the DNA bound to the glass surface, and regeneration of the hydroxyl group on the glass surface was achieved by the following UV/ozone treatment. With no further treatment, the same construction steps were repeated for the sensor to detect SARS-CoV-2 cDNA. Based on one-way ANOVA statistical analysis, it was confirmed that the differences of all measured capacitance data in each repeated cycle were not statistically significant (Fig. 3D), with p-value higher than 0.05. More importantly, the capacitance change (ΔC) remained constant within a range of ~2 nF when reusing the sensors, retaining excellent sensitivity across the recycling (Fig. 3E and supplementary Fig. 5).

4. Conclusions

In this study, a rapid, low-cost capacitive sensor for the sensitive detection of SARS-CoV-2 cDNA was developed. The results demonstrated that the capacitance changed upon the introduction of the target SARS-CoV-2 analyte to our constructed sensor with no significant cross-reactivity with SARS-CoV. The formation of dsDNA via molecular-level hybridization was verified by exhaustive electrical and optical surface analysis. The recyclability was also demonstrated by the regeneration of the glass surface after a simple construction process, allowing for their

reuse in low-resource settings. Owing to high sensitivity and specificity (Supplementary Table 2), the reported sensors have great potential in practical use and commercialization as point-of-care diagnostics for COVID-19.

Credit author statement

Chuljin Hwang: Data curation, Visualization, Investigation. **Nakkyun Park**: Data curation, Formal analysis, Investigation. **Eun Seong Kim**: Resources. **Miran Kim**: Validation. **Su Dong Kim**: Funding acquisition, Conceptualization. **Sungjun Park**: Methodology, Writing – Review & Editing. **Nam Young Kim**: Validation, Resources. **Joo Hee Kim**: Project administration, Conceptualization, Writing – Review & Editing.

Declaration of competing interest

The authors declare that they have no known competing financial interests or personal relationships that could have appeared to influence the work reported in this paper.

Acknowledgements

This research was supported by the Ministry of Food and Drug Safety (Program No. 21153MFDS431). This work was also supported by the new faculty research fund of Ajou University and a research grant (NRF-2020R1F1A1073564, 2018R1A6A1A03025242 and 2018R1D1A1A09083353) from National Research Foundation (NRF) funded by the Ministry of Science and ICT, Korea.

Appendix A. Supplementary data

Supplementary data related to this article can be found at https://doi.org/10.1016/j.bios.2021.113177.

References

Albalá, R., Olmos, D., Aznar, A.J., Baselga, J., González-Benito, J., 2004. Fluorescent labels to study thermal transitions in epoxy/silica composites. J. Colloid Interface Sci. 277, 71–78. https://doi.org/10.1016/j.jcis.2004.04.018.

Cascella, M., Rajnik, M., Cuomo, A., Dulebohn, S.C., Di Napoli, R., 2020. Features, evaluation, and treatment of coronavirus. In: StatPearls. StatPearls Publishing, Treasure Island (FL).

Chaudhary, S., Kamra, T., Uddin, K.M.A., Snezhkova, O., Jayawardena, H.S.N., Yan, M., Montelius, L., Schnadt, J., Ye, L., 2014. Controlled short-linkage assembly of functional nano-objects. Appl. Surf. Sci. 300, 22–28. https://doi.org/10.1016/j.apsusc.2014.01.174.

Chen, X., Liu, C., Hughes, M.D., Nagel, D.A., Hine, A.V., Zhang, L., 2015. EDC-mediated oligonucleotide immobilization on a long period grating optical biosensor. J. Biosens. Bioelectron. 6.

Chowell, G., Dhillon, R., Srikrishna, D., 2020. Getting to zero quickly in the 2019-nCov epidemic with vaccines or rapid testing. medRxiv. https://doi.org/10.1101/2020.02.03.20020271, 2020.02.03.20020271.

Corman, V.M., Landt, O., Kaiser, M., Molenkamp, R., Meijer, A., Chu, D.K., Bleicker, T., Brünink, S., Schneider, J., Schmidt, M.L., Mulders, D.G., Haagmans, B.L., van der Veer, B., van den Brink, S., Wijsman, L., Goderski, G., Romette, J.-L., Ellis, J., Zambon, M., Peiris, M., Goossens, H., Reusken, C., Koopmans, M.P., Drosten, C., 2020. Detection of 2019 novel coronavirus (2019-nCoV) by real-time RT-PCR. Euro Surveill. 25, 2000045. https://doi.org/10.2807/1560-7917.ES.2020.25.3.2000045.

Cuervo, A., Dans, P.D., Carrascosa, J.L., Orozco, M., Gomila, G., Fumagalli, L., 2014. Direct measurement of the dielectric polarization properties of DNA. Proc. Natl. Acad. Sci. U. S. A. 111, E3624–E3630. https://doi.org/10.1073/pnas.1405702111.

Dufva, M., 2005. Fabrication of high quality microarrays. Biomol. Eng. 22, 173–184. https://doi.org/10.1016/j.bioeng.2005.09.003.

Elder, R.M., Jayaraman, A., 2013. Structure and thermodynamics of ssDNA oligomers near hydrophobic and hydrophilic surfaces. Soft Matter 9, 11521. https://doi.org/10.1039/c3sm50958c.

Fan, Z., Zhi, C., Wu, L., Zhang, P., Feng, C., Deng, L., Yu, B., Qian, L., 2019. UV/Ozone-Assisted rapid formation of high-quality tribological self-assembled monolayer. Coatings 9, 762. https://doi.org/10.3390/coatings9110762.

Faria, H.A.M., Zucolotto, V., 2019. Label-free electrochemical DNA biosensor for zika virus identification. Biosens. Bioelectron. 131, 149–155. https://doi.org/10.1016/j.bios.2019.02.018.

Gunda, N.S.K., Singh, M., Norman, L., Kaur, K., Mitra, S.K., 2014. Optimization and characterization of biomolecule immobilization on silicon substrates using (3-aminopropyl)triethoxysilane (APTES) and glutaraldehyde linker. Appl. Surf. Sci. 305, 522–530. https://doi.org/10.1016/j.apsusc.2014.03.130.

Ilkhani, H., Farhad, S., 2018. A novel electrochemical DNA biosensor for Ebola virus detection. Anal. Biochem. 557, 151–155. https://doi.org/10.1016/j.ab.2018.06.010.

Islam, A., Ahmed, A., Naqvi, I.H., Parveen, S., 2020. Emergence of deadly severe acute respiratory syndrome coronavirus-2 during 2019–2020. VirusDisease 31, 128–136. https://doi.org/10.1007/s13337-020-00575-1.

Jang, L.-S., Liu, H.-J., 2009. Fabrication of protein chips based on 3-aminopropyltriethoxysilane as a monolayer. Biomed. Microdevices 11, 331–338. https://doi.org/10.1007/s10544-008-9239-7.

Kyaw, H.H., Al-Harthi, S.H., Sellai, A., Dutta, J., 2015. Self-organization of gold nanoparticles on silanated surfaces. Beilstein J. Nanotechnol. 6, 2345–2353. https://doi.org/10.3762/bjnano.6.242.

Layqah, L.A., Eissa, S., 2019. An electrochemical immunosensor for the corona virus associated with the Middle East respiratory syndrome using an array of gold nanoparticle-modified carbon electrodes. Microchim. Acta 186, 224. https://doi.org/10.1007/s00604-019-3345-5.

Macambira, C.N., Agopian, P.G.D., Martino, J.A., 2018. Influence of channel silicon thickness and biological material permittivity on nTFET biosensor. In: 2018 33rd Symposium on Microelectronics Technology and Devices (SBMicro). Presented at the 2018 33rd Symposium on Microelectronics Technology and Devices (SBMicro), pp. 1–4. https://doi.org/10.1109/SBMicro.2018.8511580.

Mishra, S., Kim, E.-S., Sharma, P.K., Wang, Z.-J., Yang, S.-H., Kaushik, A.K., Wang, C., Li, Y., Kim, N.-Y., 2020. Tailored biofunctionalized biosensor for the label-free sensing of prostate-specific antigen. ACS Appl. Bio Mater. 3, 7821–7830. https://doi.org/10.1021/acsabm.0c01002.

Olmos, D., Aznar, A.J., Baselga, J., González-Benito, J., 2003. Kinetic study of epoxy curing in the glass fiber/epoxy interface using dansyl fluorescence. J. Colloid Interface Sci. 267, 117–126. https://doi.org/10.1016/S0021-9797(03)00620-9.

Rashid, J.I.A., Yusof, N.A., 2017. The strategies of DNA immobilization and hybridization detection mechanism in the construction of electrochemical DNA sensor: a review. Sens. Bio-Sens. Res. 16, 19–31. https://doi.org/10.1016/j.sbsr.2017.09.001.

Rothe, C., Schunk, M., Sothmann, P., Bretzel, G., Froeschl, G., Wallrauch, C., Zimmer, T., Thiel, V., Janke, C., Guggemos, W., Seilmaier, M., Drosten, C., Vollmar, P., Zwirglmaier, K., Zange, S., Wölfel, R., Hoelscher, M., 2020. Transmission of 2019-nCoV infection from an asymptomatic contact in Germany. N. Engl. J. Med. 382, 970–971. https://doi.org/10.1056/NEJMc2001468.

Schrader, A.M., Monroe, J.I., Sheil, R., Dobbs, H.A., Keller, T.J., Li, Y., Jain, S., Shell, M.S., Israelachvili, J.N., Han, S., 2018. Surface chemical heterogeneity modulates silica surface hydration. Proc. Natl. Acad. Sci. U. S. A. 115, 2890–2895. https://doi.org/10.1073/pnas.1722263115.

Seo, G., Lee, G., Kim, M.J., Baek, S.-H., Choi, M., Ku, K.B., Lee, C.-S., Jun, S., Park, D., Kim, H.G., Kim, S.-J., Lee, J.-O., Kim, B.T., Park, E.C., Kim, S.I., 2020. Rapid detection of COVID-19 causative virus (SARS-CoV-2) in human nasopharyngeal swab specimens using field-effect transistor-based biosensor. ACS Nano 14, 5135–5142. https://doi.org/10.1021/acsnano.0c02823.

Sharfstein, J.M., Becker, S.J., Mello, M.M., 2020. Diagnostic testing for the novel coronavirus. J. Am. Med. Assoc. 323, 1437–1438. https://doi.org/10.1001/jama.2020.3864.

Singhal, C., Khanuja, M., Chaudhary, N., Pundir, C.S., Narang, J., 2018. Detection of chikungunya virus DNA using two-dimensional MoS 2 nanosheets based disposable biosensor. Sci. Rep. 8, 7734. https://doi.org/10.1038/s41598-018-25824-8.

Syga, Ł., Spakman, D., Punter, C.M., Poolman, B., 2018. Method for immobilization of living and synthetic cells for high-resolution imaging and single-particle tracking. Sci. Rep. 8, 13789. https://doi.org/10.1038/s41598-018-32166-y.

Tsouti, V., Boutopoulos, C., Zergioti, I., Chatzandroulis, S., 2011. Capacitive microsystems for biological sensing. Biosens. Bioelectron. 27, 1–11. https://doi.org/10.1016/j.bios.2011.05.047.

Wang, B., Huang, Y., Liu, L., 2006. Effect of solvents on adsorption of phenolic resin onto γ-aminopropyl-triethoxysilane treated silica fiber during resin transfer molding. J. Mater. Sci. 41, 1243–1246. https://doi.org/10.1007/s10853-005-4226-3.

Wang, J., Wang, H., Wang, Y., Li, J., Su, Z., Wei, G., 2014. Alternate layer-by-layer assembly of graphene oxide nanosheets and fibrinogen nanofibers on a silicon substrate for a biomimetic three-dimensional hydroxyapatite scaffold. J. Mater. Chem. B 2, 7360–7368. https://doi.org/10.1039/C4TB01324G.

Wang, L., Veselinovic, M., Yang, L., Geiss, B.J., Dandy, D.S., Chen, T., 2017. A sensitive DNA capacitive biosensor using interdigitated electrodes. Biosens. Bioelectron. 87, 646–653. https://doi.org/10.1016/j.bios.2016.09.006.

Watson, H., Norström, A., Torrkulla, Å., Rosenholm, J., 2001. Aqueous amino silane modification of E-glass surfaces. J. Colloid Interface Sci. 238, 136–146. https://doi.org/10.1006/jcis.2001.7506.

Whitesides, G.M., 2006. The origins and the future of microfluidics. Nature 442, 368–373. https://doi.org/10.1038/nature05058.